Hannula, Pyry Mikko; Pletincx, Sven; Janas, Dawid; Yliniemi, Kirsi; Hubin, Annick; Lundström, Mari

Controlling the deposition of silver and bimetallic silver/copper particles onto a carbon nanotube film by electrodeposition-redox replacement

Published in:
Surface and Coatings Technology

DOI:
10.1016/j.surfcoat.2019.05.085

Published: 25/09/2019

Document Version
Publisher's PDF, also known as Version of record

Surface & Coatings Technology 374 (2019) 305–316

Contents lists available at ScienceDirect

Surface & Coatings Technology

journal homepage: www.elsevier.com/locate/surfcoat

Controlling the deposition of silver and bimetallic silver/copper particles onto a carbon nanotube film by electrodeposition-redox replacement

Pyry-Mikko Hannula[a,*], Sven Pletincx[b], Dawid Janas[c], Kirsi Yliniemi[a], Annick Hubin[b], Mari Lundström[a]

[a] Aalto University, Department of Chemical and Metallurgical Engineering, School of Chemical Engineering, Vuorimiehentie 2, 02150 Espoo, Finland
[b] Department of Materials and Chemistry, Research Group Electrochemical and Surface Engineering (SURF), Vrije Universiteit Brussel, Pleinlaan 2, 1050 Brussels, Belgium
[c] Department of Chemistry, Silesian University of Technology, B. Krzywoustego 4, 44-100 Gliwice, Poland

ARTICLE INFO

Keywords:
Electrodeposition
Redox replacement
Bimetallic
Particle
Copper
Silver

ABSTRACT

The electrodeposition-redox replacement (EDRR) process was studied to control the creation of copper and silver containing particles on the surface of a carbon nanotube film. Synthetic solutions simulating typical hydrometallurgical copper electrolysis process solutions (40 g/L Cu, 120 g/L H_2SO_4) with different dilute concentrations of silver (1–10 ppm) were utilized as the source for particle deposition and recovery. Such process solutions are currently underutilized for use as a potential source for the deposition of noble particles. The effect of deposition voltage, deposition time, stirring, and redox replacement time between deposition pulses were investigated as the parameters affecting the morphology and composition of the deposited particles as well as deposition kinetics. The results showed that pure copper particles can be deposited when the redox replacement time between deposition pulses is very short (t = 2 s). By increasing the redox replacement time (t = 50 s and more) the original copper particle composition transforms into a core-shell structure with an outer layer predominately consisting of silver or a bimetallic mix of copper and silver, depending on the deposition conditions. The bimetallic Cu/Ag particle size could be controlled from 200 to 840 nm by the applied deposition voltage. At high redox replacement times (t = 150 s and more) the resulting particles were shown to be pure silver with a small diameter from 100 to 250 nm.

1. Introduction

In this paper a method is presented for depositing either Ag or Cu/Ag particles on carbon nanotube (CNT) films from solutions mimicking hydrometallurgical copper process solutions, such as those used in copper electrorefining and electrowinning. In the industrial solutions used in these hydrometallurgical processes, depending on the plant operation, trace amounts of noble elements such as silver (in the ppm range) are accompanied by a considerably higher concentration of less noble metals (in the g/L range), such as copper, iron, nickel [1]. Currently utilized silver recovery processes from such dilute solutions include several different methods such as cementation [2–5], chemical methods [6], precipitation [7], adsorption [8], membrane filtration [9] and electrowinning [10–12]. The typical issues when recovering silver from dilute industrial effluents by any method are in the solution complexity, high cost, high consumption of chemicals or high energy consumption of the process [13]. Unlike with the novel method presented here, the currently utilized removal processes do not directly produce high added-value surfaces with desired silver particle composition and distribution, but are rather focused in the effective removal of silver from the solution.

In the field of electrochemistry, redox replacement reactions have been used to create precise monolayers of metals on wanted substrates in a so-called surface-limited redox replacement (SLRR) process [14–18]. This method has traditionally utilized underpotential deposition in a two-step procedure, mostly in two different deoxygenated solutions consisting of noble and non-noble elements respectively, but has also been conducted within a single solution containing both elements [19,20]. The composition of the solutions used in these studies is carefully adjusted so that the redox replacement process can be precisely controlled in order to produce surfaces of desired composition.

The electrodeposition- redox replacement (EDRR) process is a versatile one-step approach for creating porous deposits or (nano)particles from a single solution containing both the noble and non-noble elements. Recently, the EDRR process has been utilized to control the deposition of Pt/Ni [21] particles and to recover films of valuable

* Corresponding author.
E-mail addresses: pyry.hannula@aalto.fi (P.-M. Hannula), mari.lundstrom@aalto.fi (M. Lundström).

https://doi.org/10.1016/j.surfcoat.2019.05.085
Received 8 April 2019; Received in revised form 13 May 2019; Accepted 29 May 2019
Available online 30 May 2019

metals such as Au [22] and Ag [23] from various industrial waste sources. Silver particles, and their more economical alternative bimetallic copper-silver particles, have been widely utilized in different applications such as electronics [24–28] catalysts, [29–33] and antibacterial materials [34–37]. On the other hand, carbon nanotube based materials have been utilized widely in electrochemical applications due to their high surface area and conductivity [33,36,38,39]. For instance, copper and silver particles supported on carbon nanotube (CNT) materials have been utilized to produce functional materials for applications as sensors [38,39], catalysts [33,40], antibacterial materials [34,36] and conductors [41–45]. Thus, utilizing a CNT film as the electrode material for the EDRR process offers the possibility of producing a functional surface of copper and silver nanoparticles directly from the industrial copper process solution. The composition of the typical industrial copper electrolysis solutions used in this study are not optimized for silver particle deposition and have therefore not been traditionally considered as a potential source for the creation of different types of CNT-Cu/Ag surfaces.

In this communication, the EDRR process was studied in a solution with composition similar to those used in industrial copper electrolysis, i.e. containing dilute amounts of silver (1–10 ppm) and a high concentration of Cu (40 g/L). By controlling the various EDRR parameters the composition and morphology of deposited particles on carbon nanotube films could be tuned in order to produce a high-added value surface. Combining the techniques of Field Emission Scanning Electron Microscopy with Energy Dispersive X-ray spectroscopy (FE-SEM & EDS), X-ray Photoelectron Spectroscopy (XPS), Field Emission Auger Electron Spectroscopy (FE-AES) with electrochemical data, such as open circuit potential (OCP) transient values allowed for the comprehensive study of the resulting deposits by the EDRR method. It was found that the deposits could be tuned from pure Cu to bimetallic Cu/Ag to highly pure Ag particles.

2. Experimental and methods

A three-electrode cell with a volume of 200 cm^3 was used at room temperature in the electrochemical experiments. The experiments were controlled by an Autolab PG 302 potentiostat with Nova 2.1 software. The reference electrode was a silver chloride (Ag/AgCl) in a 1 M sodium sulphate (Na_2SO_4, EMSURE, Merck) salt bridge to avoid possible contamination of the electrolyte by chlorides. The counter electrode was a Ti/RuO_2 mesh anode with surface area an order of magnitude larger than the geometrical working electrode area. The counter electrode was in a U-shape around the working electrode to ensure an even current distribution during experiments. The experiments were conducted in a solution with background composition of 40 g/L (0.63 M) of Cu from copper sulphate pentahydrate ($CuSO_4{\cdot}5H_2O$, EMSURE, Merck) and 120 g/L (1.2 M) of sulphuric acid (H_2SO_4, Analytical reagent grade, Fisher Chemical), hereby called the copper process solution. The Ag concentration in copper process solutions was varied from 1 to 10 ppm by diluting silver AAS standard (TraceCERT®, 39361, Sigma-Aldrich) with original concentration of 1000 ppm Ag and 2 wt-% HCl. The solutions were made with Milli-Q water. The composition and pH of the utilized solutions are selected to mimic the typical composition of copper electrolysis process solutions [2,3,46]. The working electrode was a free standing CNT film produced by the liquid suspension method, shown in [47]. These films exhibit hydrophilic characteristics [48,49], making them suitable for use as electrodes for aqueous solutions. CNT film samples used as the working electrode were cut with a surgical blade to dimensions of ca. 1 × 2.5 cm. Due to the rigid nature of the CNT film a crocodile clip was attached directly onto the film to pass current during the experiments. After deposition the samples were immediately removed from the solution and carefully rinsed with DI-water before placed in a desiccator. The reported average open circuit potential (OCP) values have been averaged from the OCP value of the working electrode at the end of each cycle during the EDRR process. The error reported with the average OCP value is one standard deviation.

Field Emission Scanning Electron Microscopy (FE-SEM) was done with a JEOL JSM-7100F, equipped with energy dispersive X-ray spectroscopy (EDS) to image and analyze the sample morphology and composition. The acceleration voltage during imaging and EDS analysis was 15 kV. At least 10 particles per sample were analyzed by EDS from randomly selected points along the surface. The reported EDS Cu:Ag wt-% ratios are calculated by the ratio of the average wt-% of Cu and Ag of the analyzed particles. The wt-% ratios were calculated for all analyzed samples to compare the trends of compositional changes between deposits. ImageJ software was used to analyze the particle sizes from SEM images of 5000 (x5k) and 30,000 (x30k) magnifications with a minimum of 100 particle measurements per sample. The error reported with the average diameter is one standard deviation.

X-ray photoelectron spectroscopy (XPS) measurements were done to measure CNT films with different copper and silver surface compositions up to ca. 10 nm in depth with a PHI-5600ci (Physical Electronics) utilizing an Al Kα monochromatic X-ray source (1486.71 eV photon energy) with a spot diameter of 800 μm for scanning large areas of the CNT film surface. Each survey was conducted for 12 individual acquisition scans (14 min of total measuring time per spectrum) and 3 surveys were taken of each sample at different locations. The vacuum in the analysis chamber was lower than 1×10^{-9} Torr. Survey scans were recorded with a pass energy of 187.85 eV and energy step size of 0.8 eV. The XPS data was analyzed with PHI Multipak software (V9.5). Non-deposited elements on some of the CNT film samples included Cl, S, Si and N as a contamination. Survey scans for the pure CNT film and CNT film with Cu, Cu/Ag and Ag particles are shown in Fig. S1. Relative recovery values of Ag are calculated for samples with high replacement time by dividing the total charge spent during the EDRR electrodeposition stages by the average concentration of Ag (atomic %, at-%) at the CNT film surface. Importantly, in these samples no Cu could be detected in the XPS and the particles were highly pure Ag by EDS. The relative recovery efficiency of Ag was calculated using the surface coverage of Ag (at.%) on the film surface from the XPS surveys and the charge density (mC/cm^2) during deposition of copper particles. The relative recovery efficiency can be estimated by dividing the Ag (at.%) amount (from three measurements on separate locations) on each sample by the total charge density (mC/cm^2) during deposition pulses on that sample.

Field emission Auger electron spectroscopy (FE-AES) was done with a JEOL JAMP-9500F to investigate the composition profile of individual particles on the CNT film by utilizing argon ion sputtering. The sputtering rate was a constant 3.3 nm/min (according to the sputtering rate of SiO_2) for all samples.

As carbon-based material itself is known to be able to support redox replacement of some noble elements, such as Cu [50] and Ag [51], a reference test was made to observe that our results are truly due to the EDRR process and no other redox replacement phenomena stemming from the working electrode material. A CNT film sample was immersed in a solution of 40 g/L of Cu, 120 g/L of H_2SO_4 and 100 ppm of Ag (ten times higher Ag concentration than in our EDRR experiments) for one hour and then rinsed with DI water. XPS analysis showed that after this time no spontaneously deposited Cu or Ag could be found at the surface.

3. Results and discussion

3.1. Redox replacement between copper and silver

The redox replacement reaction between copper and silver in a copper process solution is thermodynamically possible due to the difference in reduction potentials between this reduction - oxidation pair. The electrode potential values for the investigated copper process solution were calculated with the Nernst equation from the

concentrations of 40 g/L Cu and 10 ppm Ag:

$$Cu^{2+} + 2e^- \rightarrow Cu(s)\ E^1_{eq} = 0.331\ V\ vs.\ SHE \quad (1)$$

$$Ag^+ + e^- \rightarrow Ag(s)\ E^2_{eq} = 0.561\ V\ vs.\ SHE \quad (2)$$

The overall reaction occurring during the redox replacement step can be described as:

$$Cu(s) + 2Ag^+(aq) \rightarrow 2Ag(s) + Cu^{2+}\ E^2_{eq} - E^1_{eq} = 0.230\ V \quad (3)$$

where each copper atom is being replaced by two silver atoms. The difference in the calculated theoretical electrode potentials is then 0.230 V in the solution employed in this study.

To observe the redox replacement reaction in our solution in its basic form between copper and silver, the following experiment was conducted: a thick bulk copper surface on a CNT film sample was deposited at −0.1 V vs. Ag/AgCl for 1200 s in a copper process solution without Ag, and then this Cu-CNT film was immersed in a copper process solution containing 10 ppm Ag for 3000 s. As with all experiments, the solutions were not purged free of dissolved oxygen and thus some corrosion of the bulk copper was expected to occur simultaneously with the redox replacement. The resulting surfaces are shown in Fig. 1. In Fig. 1a, the surface of electrodeposited pure bulk copper is shown. After immersion in 10 ppm silver containing copper process solution, the copper starts to oxidize while silver particles (confirmed by EDS analysis) of ca. 100 nm diameter deposit on the remaining bulk copper surface, Fig. 1b. This result shows that in our solution with a dilute silver content and no deoxygenation, the redox replacement reaction between copper and silver is thermodynamically favored.

The redox replacement system between copper and silver in an electrolyte similar to the one utilized here, containing various concentrations of copper sulphate, sulphuric acid and silver, has been scarcely studied to date with the exception of Sulka and Jaskula [2,3]. They studied the kinetics and mechanisms of redox replacement between a solid copper plates and silver ions in a copper electrowinning electrolyte with a higher concentration of silver (between 20 and 100 ppm Ag) and ca. half the sulphuric acid concentration (0.5 M H_2SO_4) employed in our study. To summarize their work, they showed that in acidic sulphate based electrolyte silver can redox replace bulk copper in various forms. Silver deposits as particles, dendrites and solid films on the surface of existing bulk copper, depending on the applied conditions and solution composition. In solutions not purged with oxygen, the corrosion of copper occurs as a side reaction simultaneously with redox replacement. Under this condition silver was shown to deposit preferentially on existing silver due to the higher surface area of anodic sites. [2,3] It is worth noting however, that their study was not done on copper particles but instead, bulk copper plates were immersed into silver and copper containing solutions.

Pure copper particles were deposited at −0.1 V for 500 ms (n = 20) in copper process solution with 10 ppm Ag, Fig. 2a. These particles were deposited with 2 s replacement time between deposition pulses. Due to the short replacement time, no redox replacement took place (EDS Cu:Ag wt% ratio of ca. 121) and thus 2 s replacement time was considered as the reference for creating highly pure copper particles on the CNT film. The minor amount of silver detected in the particle is assumed to be due to co-deposition of silver with copper during the deposition pulse. Another reference sample was produced by immersing the pure copper particles into copper solution with 10 ppm Ag for a total of t = 3000 s and the resulting morphology is shown in Fig. 2b. The deposits produced by this traditional, non-pulsed redox replacement method, called cementation in hydrometallurgy, were mostly silver (3.6% Cu as impurity by EDS analysis) with a high degree of agglomeration and a bimetallic surface structure of copper and silver. The compiled analysis results of these particles are shown for comparison purposes, together with the results from EDRR experiments with long replacement time (Table 1).

3.2. EDRR process with long replacement time

The EDRR process for silver particle deposition is shown schematically in Fig. 3. Here, the CNT film surface is first deposited with copper particles by an electrodeposition (ED) pulse (during which a minor amount of silver will also co-deposit). The morphology and amount of the copper deposit before any redox replacement with silver can be affected by the deposition voltage and deposition time. After the deposition pulse, the system is left at open circuit potential (OCP) for a desired time, hereby called replacement time, so redox replacement reactions can take place between the deposited copper particles and silver ions in solution while no external potential or current is being applied. During this step, silver reduces on the working electrode surface while the copper deposits are oxidized and dissolved into the solution. This cycle of deposition and redox replacement is then repeated for a number of times (n) to increase the amount of metal deposits at the CNT film surface. The energy consumption of the process is related to the deposition charge during pulsing and the amount of silver recovered. The main difference between EDRR and traditional methods for performing redox replacement reactions (such as the one shown in Fig. 2b) is that in EDRR the redox replacement takes place on a small number of particles after each deposition cycle. Thus, the amount of copper replaced by silver during one EDRR cycle is considerably smaller than when replacing all copper particles at once. This is important to note as the concentration of silver and other noble metals in copper process solutions are typically very small, hence the mass transfer can affect the replacement reaction considerably.

Fig. 4 shows a typical EDRR graph obtained when forming silver

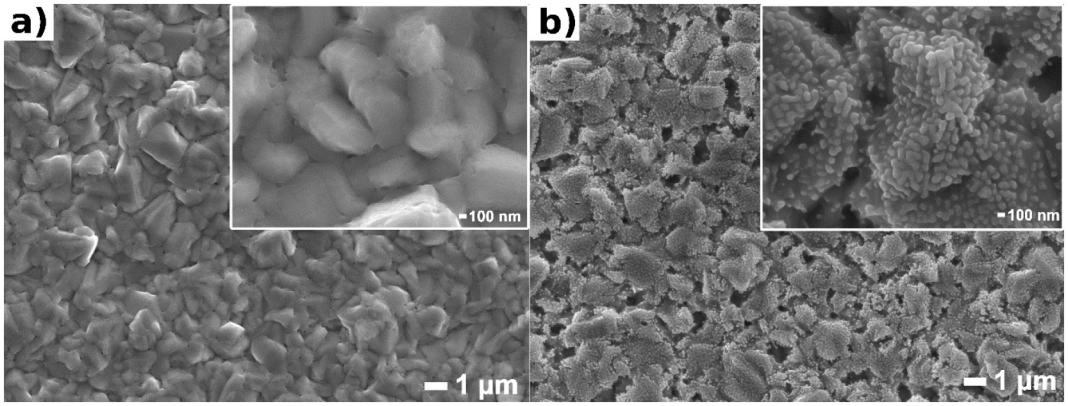

Fig. 1. SEM images of bulk copper surface deposited from pure copper process solution without any Ag (a) after redox replacement for 3000 s in copper process solution with [Ag] = 10 ppm (b).

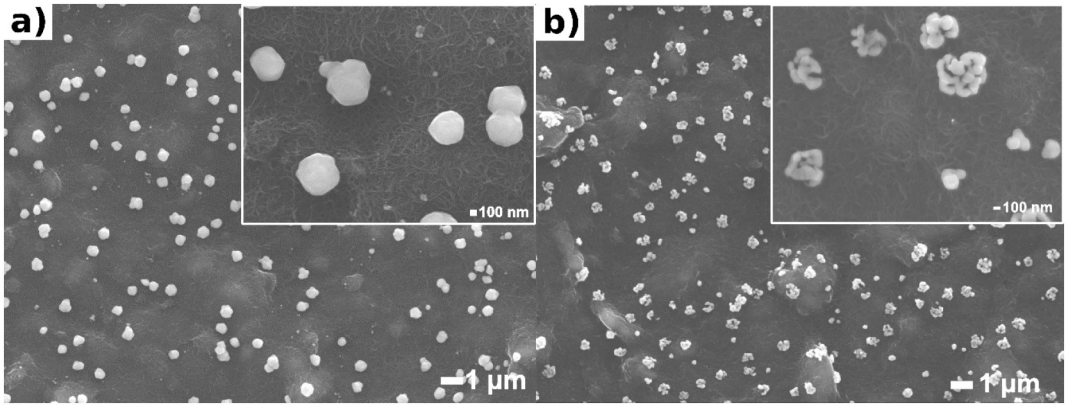

Fig. 2. SEM images of (a) copper particles deposited at −0.1 V vs. Ag/AgCl for 500 ms (2 s replacement time) in copper process solution [Ag] = 10 ppm, (b) silver particles after copper particle immersion, i.e. cementation, in [Ag] = 10 ppm copper process solution for 3000 s.

Table 1
Production and characterization of pure Ag particles by EDRR (n = 20) and cementation from copper process solution with [Ag] = 10 ppm.

Deposition potential vs. Ag/AgCl (V)	Deposition time (ms)	Replacement time (s)	EDS, Cu:Ag (wt %-ratio)	XPS, Cu:Ag (wt %-ratio)	Deposit size (nm)	Ag recovery efficiency (at.%cm^2/mC)	Average OCP vs. Ag/AgCl (mV)
−0.1	500	150	0.01	Pure Ag	247 ± 118	0.05	297 ± 0.003
−0.5	500	600	0.01	Pure Ag	207 ± 65	0.08	305 ± 1
−0.5	50	300	0.001	Pure Ag	96 ± 37	0.29	268 ± 7
Traditional redox replacement i.e. cementation		3000	0.036	Bimetallic Cu/Ag (0.4)	416 ± 102	0.04	–

particles (using ED pulse for 500 ms at −0.1 V vs. Ag/AgCl and redox replacement time of 150 s for a total of n = 20 cycles). The open circuit potential was recorded during the redox replacement step (during which no external potential or current was applied) and its increase is due to the higher nobility of silver when compared with copper.

Fig. 5 shows the silver particles obtained by EDRR on CNT film, with different deposition conditions. In Fig. 5a (20 EDRR cycles with 150 redox replacement time), the total redox replacement time was the same as for the particles in Fig. 2b (cementation reference sample with t = 3000 s redox replacement). The only difference is that in Fig. 5 the silver particles were generated by one electrodeposition pulse – redox replacement at a time, i.e. by the EDRR process. CNT film samples were also deposited with silver with parameters of −0.5 V vs. Ag/AgCl for 500 ms with 600 s replacement time and 50 ms with 300 s replacement time, Fig. 5b and Fig. 5c, respectively. In both cases the higher overpotential seemed to increase the density of the EDRR generated silver particles. This is attributed to the higher coverage and number of copper particles deposited at higher overpotential, which also leads to more homogeneous distribution of the silver particles after redox replacement has taken place. Table 1 summarizes the results of creating Ag deposits by EDRR and cementation from electrochemical measurements, SEM-EDS and XPS. The reported OCP values of the working electrode in Table 1 are the average of all values at the end of EDRR

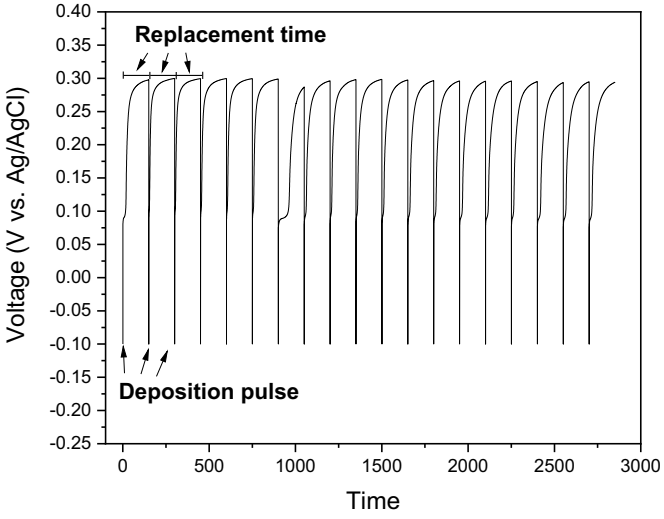

Fig. 4. Typical time-potential graph for the EDRR process (n = 20) with deposition voltage of −0.1 V vs. Ag/AgCl for 500 ms and 150 s replacement time.

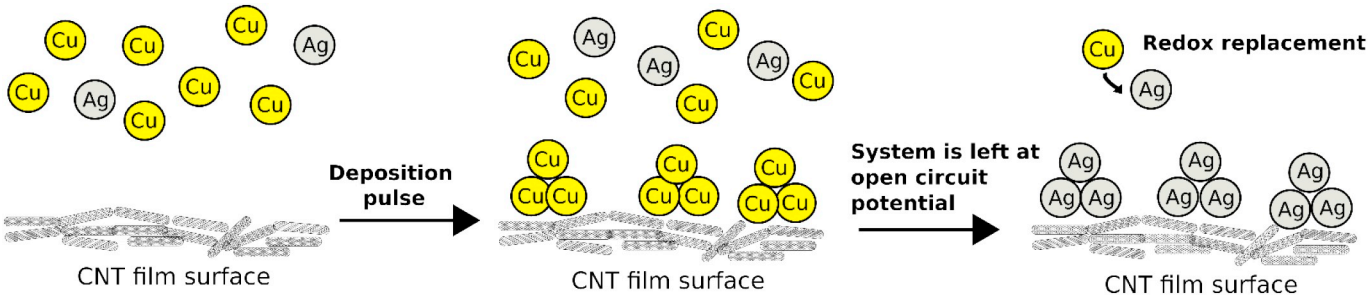

Fig. 3. Schematic for a single cycle of electrodeposition-redox replacement for creating Ag nanoparticles on CNT film.

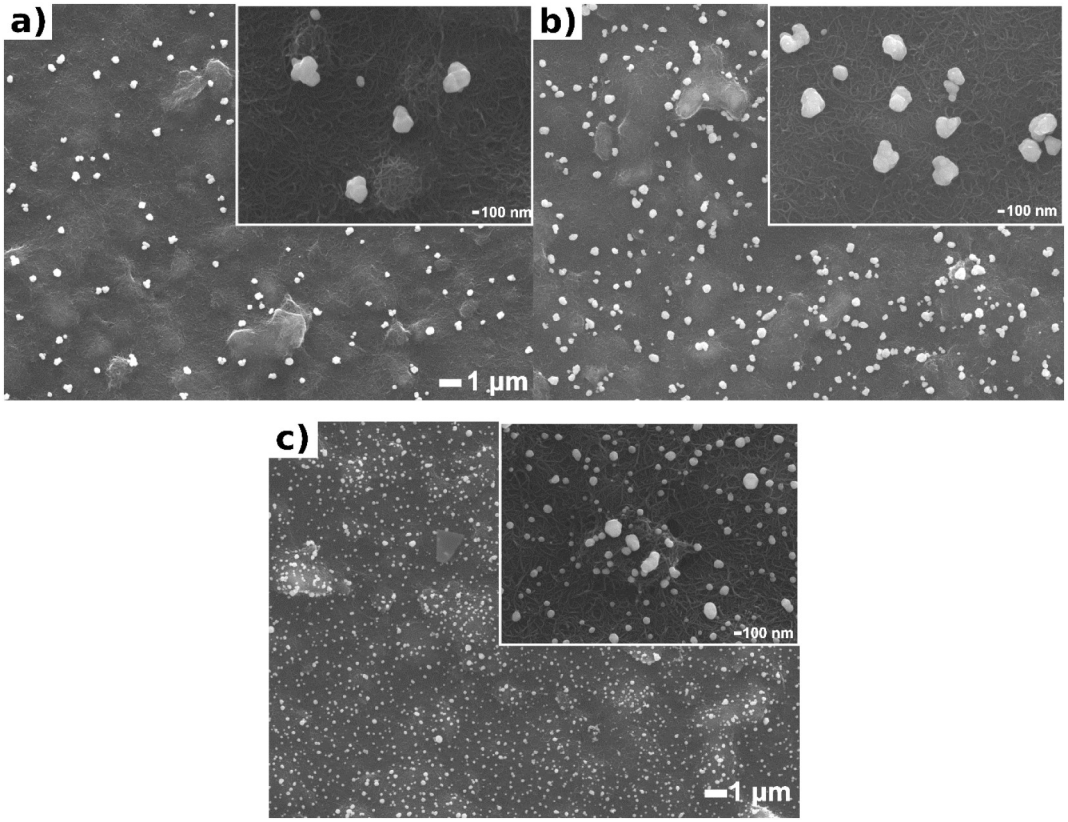

Fig. 5. SEM images of silver particles deposited by 20 EDRR cycles in 10 ppm Ag copper process solution with the parameters (a) deposition potential of −0.1 V vs. Ag/AgCl for 500 ms with 150 s of replacement time, (b) deposition potential of −0.5 V vs. Ag/AgCl for 500 ms with 600 s replacement time and (c) deposition potential of −0.5 V vs. Ag/AgCl for 50 ms with 300 s replacement time.

cycles.

The differences between silver deposits by EDRR and cementation are shown to be numerous. The silver deposits recovered by EDRR are up to ca. 4.3 times smaller, while covering the CNT film surface more homogeneously. Typical to redox replacement processes [14,17,20] some copper remains in all of the deposits, but the silver deposits recovered by EDRR were considerably higher in purity (0.1–1% Cu compared with 3.6% Cu by cementation). When comparing the silver recovery efficiencies from XPS measurements, all the EDRR experiments showed a higher amount of recovered silver by XPS surveys (0.3 to 7.3 times more) per consumed charge than by cementation. These results show that the EDRR process is an efficient and controllable way to deposit silver from metallurgical process solutions with very a dilute concentration of silver and high concentration of copper. The results for copper process solutions with even lower Ag concentration (1 ppm Ag) are reported in Table S1 and Fig. S3, which show similar trends for the creation of silver deposits.

Field Emission Auger Electron Spectroscopy (FE-AES) equipped with argon ion sputtering was used on the sample deposited at −0.1 V vs. Ag/AgCl for 500 ms with 150 s replacement time (n = 20) (same conditions as used to form pure Ag particles shown in Fig. 5a). With this technique the composition of individual particles could be observed. The particle composition profiles by sputtering time for four particles are shown Fig. 6. It has to be noted that the sputtering speed is calibrated to the sputtering rate of SiO_2 and will thus vary slightly from the actual sputtering depth of pure silver. All the particles show a pure silver structure throughout the particles with no copper peak being visible. This result further confirms the high purity of the particles as shown by the EDS and XPS results. It is assumed that the decrease in the silver peak intensity for the 1st particle after 1500 s is due to the sputtering reaching the bottom of the silver particle as this particle was also the smallest of the four particles analyzed. Importantly, no oxygen could be detected on any of the deposits.

3.3. EDRR process with low replacement time

Particles (in the size range of 10 nm to 10 µm) with a Cu core and Ag shell as well as bimetallic Cu/Ag particles (with a mixed composition of both elements) have been previously investigated for a variety of applications in the form of powders [24–28,35,37,52] or as particles supported on another material [29–32]. Particles containing both Cu and Ag are often used due to their lower cost, while maintaining or improving on the properties of pure Ag and Cu. The simplified process often utilized in literature for the creation of these particles is by cementation, i.e. immersion of existing copper powders or copper particles pre-deposited on a substrate, in a silver containing solution. The utilized solutions are typically synthetic and purged free from oxygen while containing additives such as oleylamine, sodium citrate and EDTA to control the particle synthesis. It is known that the amount of redox replaced silver is a function of the replacement time and its structure is related to the morphology of the copper particles being replaced. The concentration of silver ions to copper particles is also an important parameter due to its effect on the overall redox replacement process and is for this reason typically optimized to ensure specific type of particle formation [32,52]. In our study, the solution composition was not optimized for bimetallic or pure silver recovery, rather a selected range of EDRR parameters were investigated so as to tune the deposition of various types of particles.

To create Cu/Ag particles by the EDRR method from the copper process solutions containing 10 ppm Ag the replacement time between deposition pulses was decreased so as not to redox replace all of the deposited copper. Due to the short replacement time the silver could not redox replace all of the existing copper but both elements remained in the deposited particles. Three different deposition conditions were

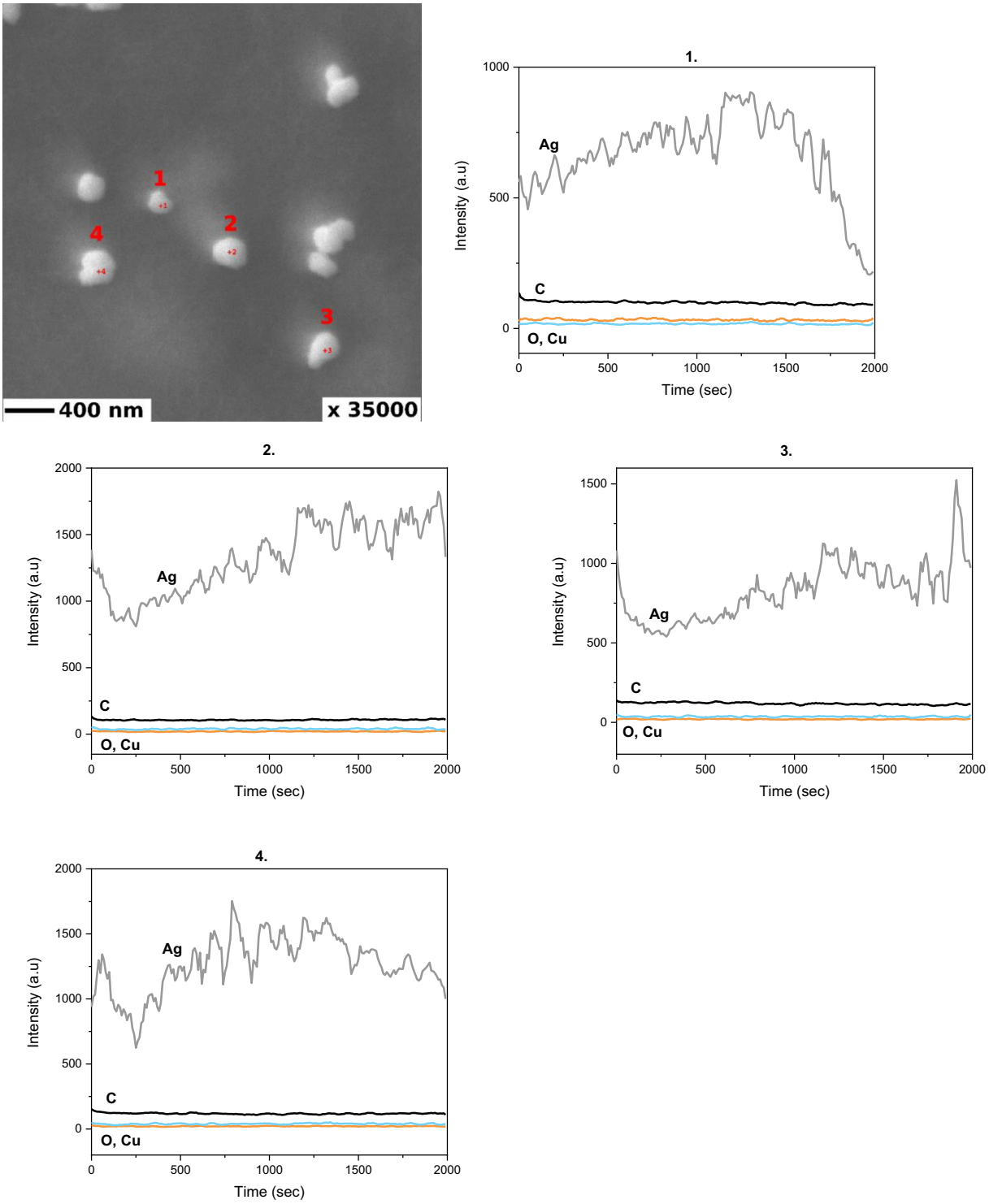

Fig. 6. Field emission Auger electron spectroscopy depth profiles of particles from copper process solution with [Ag] = 10 ppm for deposition of −0.1 V vs. Ag/AgCl for 500 ms and 150 s replacement time.

investigated: −0.1 V vs. Ag/AgCl for 500 ms, −0.5 V vs. Ag/AgCl 500 ms and −0.5 V vs. Ag/AgCl for 50 ms. The replacement time between pulses was varied from 2 to 300 s to produce CNT films with different deposit sizes and compositions. The morphologies of deposits on CNT films after EDRR (n = 20) in this low replacement time regime are shown in Fig. 7, where the replacement time is shown in the upper left corner. Compiled results of EDS analysis, XPS surveys, OCP values and deposit sizes are also shown in Table 2. The reported average OCP values in Table 2 are the average of recorded values at the end of EDRR cycles. XPS analysis was also conducted on all samples to observe for possible differences between the surface composition (analysis depth up to ca. 10 nm) and bulk composition (from EDS analysis) of the CNT film prepared with different types of Cu/Ag deposits.

Tests with 2 s replacement time were done to observe the resulting morphology during deposition of pure Cu particles with very low silver loading as the short replacement time does not allow for redox replacement to take place (EDS Cu:Ag wt% ratios >120). As expected, all the copper particles deposited with 2 s replacement time show a pure

copper surface from XPS surveys no matter the deposition conditions. Thus, these particles show the typical morphology of copper deposited before redox replacement has occurred within a single cycle of EDRR. The copper particles deposited with −0.1 V and −0.5 V vs. Ag/AgCl for 500 ms are round with some particles growing together, typical of pulsed electrodeposition [53]. For deposition with −0.5 V vs. Ag/AgCl for 50 ms, the copper deposit morphology is clearly different, exhibiting a mixed structure of cuboidal and round particles, similar to previously published results [32,54]. The deposition charges during deposition of pure copper particles with 2 s replacement time are shown in Fig. 8. Due to the high overpotential and time, deposition at −0.5 V vs. Ag/AgCl for 500 ms deposited up to 10 times more copper in a single electrodeposition pulse (equaling ca. 50 monolayers of copper, assuming a copper monolayer charge of 324 μC/cm^2 [55]) than the other conditions. The deposition charge in Fig. 8 is assumed to be increasing in successive cycles due to an increase in the electroactive surface area as the electrical conductivity and surface roughness increase with the amount of deposit [17,18,56].

The Cu:Ag wt%-ratio evolution from EDS analysis at different replacement times is plotted in Fig. 9. As expected, when increasing the replacement time the silver loading onto the CNT film working electrode increased in all cases as more copper was replaced with silver and possibly as some copper was corroded. Thus, the Cu:Ag wt%-ratio obtained by EDRR shows a wide range of possible deposit compositions as a function of the replacement time. All of the OCP values show an increase as the amount of silver, i.e. replacement time, is increased due to the higher nobility of silver, consistent with previous work on SLRR with Pb and Pt [20]. The diameter of the deposits also show a trend of decreasing as a function of the replacement time, as multiple silver particles are formed from a single original copper particle [32,52].

According to the XPS results, all samples with 50 s replacement time and higher have significant amounts of silver on the surface of copper particles (surfaces of either pure Ag or bimetallic Cu/Ag).For instance, with 50 s replacement time the samples deposited at −0.1 V vs. Ag/

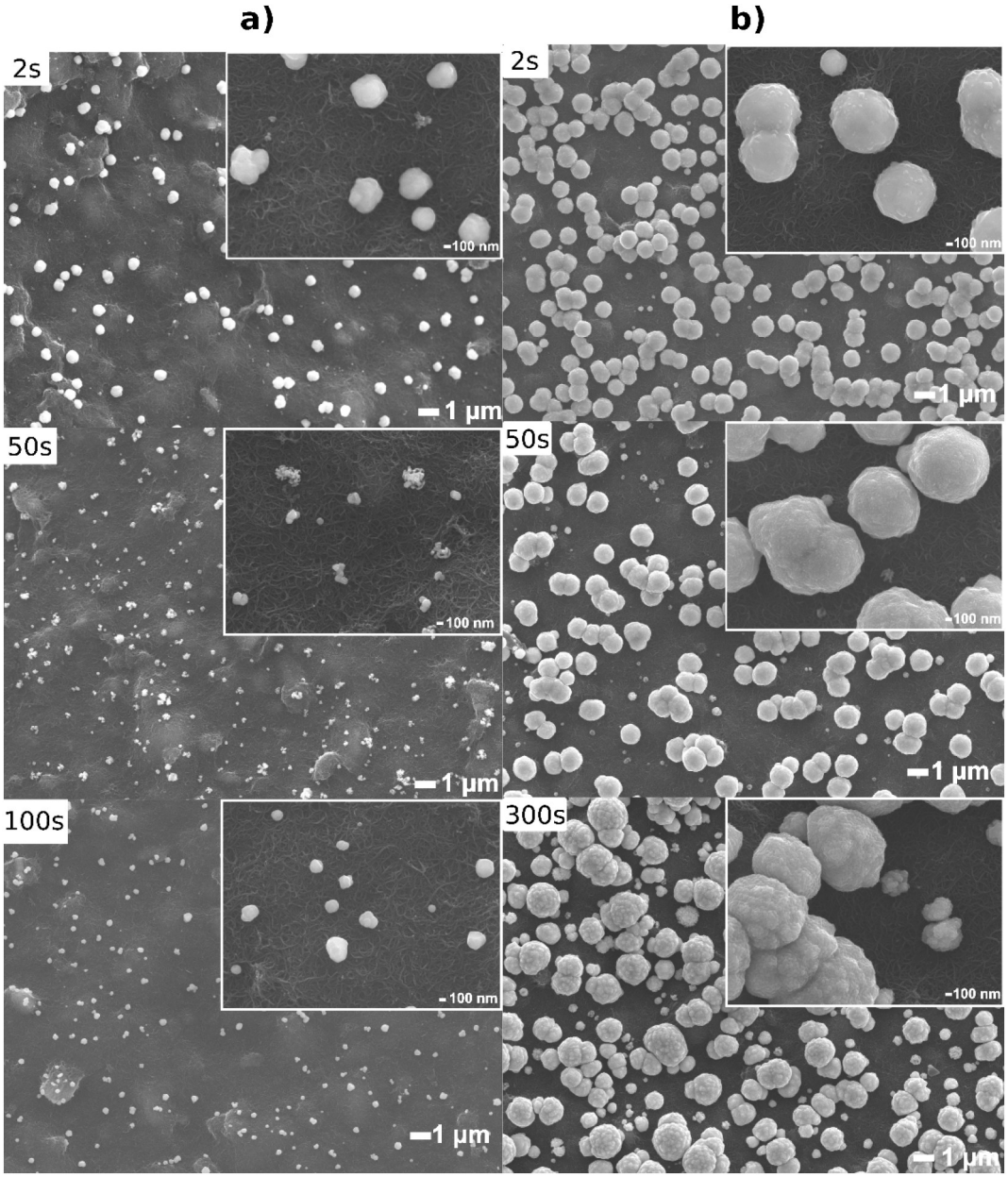

Fig. 7. SEM images of Cu/Ag particle morphology after 20 cycles of EDRR in [Ag] = 10 ppm copper process solution and different replacement times (shown in images) for (a) −0.1 V vs. Ag/AgCl for 500 ms, (b) −0.5 V vs. Ag/AgCl for 500 ms and (c) −0.5 V vs. Ag/AgCl for 50 ms.

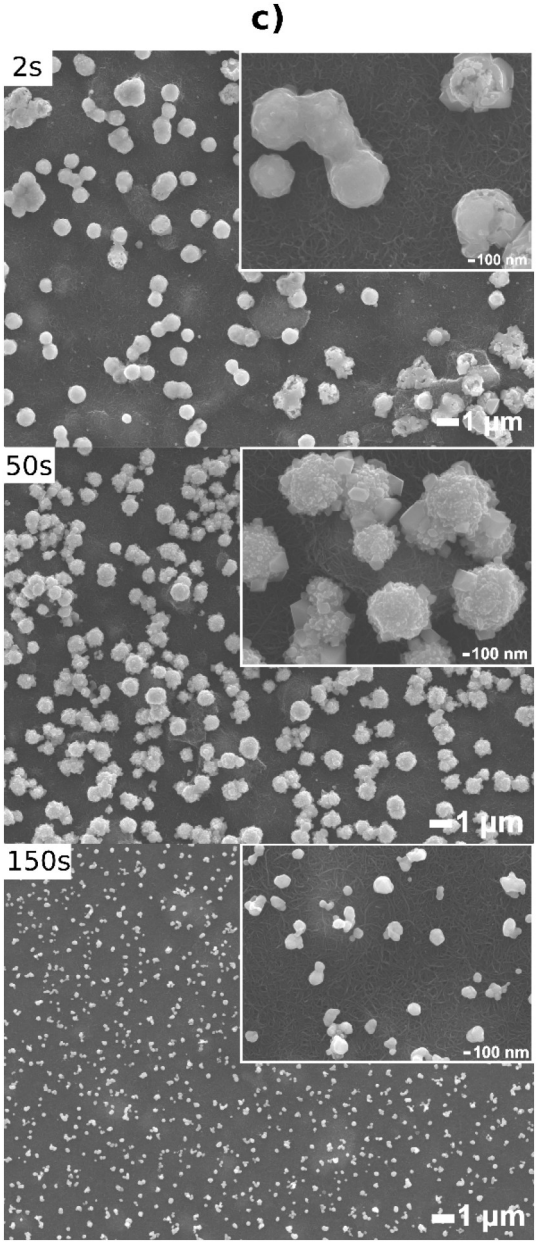

Fig. 7. (*continued*)

AgCl for 500 ms and −0.5 V vs. Ag/AgCl for 50 ms show a bimetallic surface structure of both Cu and Ag, while the sample deposited at −0.5 V vs. Ag/AgCl for 500 ms shows a pure Ag surface, i.e. core-shell structure. As the sample deposited at −0.1 V vs. Ag/AgCl for 500 ms showed the smallest copper particle size before redox replacement (and thus the highest copper surface area per particle), redox replacement was kinetically favored on the copper particles of this sample. This conclusion is also supported by the lowest Cu:Ag wt%-ratio of 6 at 50 s replacement time from EDS analysis. The bimetallic deposits of this sample, shown in Fig. 7a, exhibit a high degree of porosity/roughness due to the extensive redox replacement that has taken place. Due to the mixed growth of cuboidal and spheroidal copper particles on the CNT film when depositing at −0.5 V vs. Ag/AgCl for 50 ms (Fig. 7c), the redox replacement that occurred during the 50 s replacement time did not proceed to homogeneously cover the copper surfaces with silver. This is likely due to the differences in redox replacement rate on copper particles of mixed morphologies, which results in an uneven silver surface at low replacement times [32]. Conversely, XPS analysis of the CNT film deposited at −0.5 V vs. Ag/AgCl for 500 ms with 50 s replacement time shows deposits with a pure Ag surface. The diameter of the deposits does not show considerable decrease from the original pure copper particles at 50 s replacement time, while the Cu:Ag wt%-ratio has decreased drastically from 174 to 33 due to the increase in silver loading at the copper particle surfaces. Thus, while the bulk of the particle is at this point pure copper, the outermost layer is pure silver and the deposit is core-shell structured.

When magnetic stirring was applied (300 rpm) during the EDRR process for the sample deposited at −0.1 V vs. Ag/AgCl for 500 ms with 50 s replacement time, the mass transfer of silver to the copper surface was increased considerably, resulting in deposits with considerable higher purity than when no stirring was applied. SEM images of these deposits are shown in Fig. S2, which exhibit considerable agglomeration compared with the other pure silver deposits after long replacement times and no stirring (Fig. 5).

The sample deposited at −0.1 V for 500 ms with 50 s replacement time and no stirring was also studied with FE-AES by depth profiling to further characterize the individual deposit structures. Three depth profiles were made by argon ion sputtering coupled with elemental analysis, shown in Fig. 10. Here, two of the particles showed clear core-shell nature with the outer layer consisting of silver and the subsequent inner core of copper. The third particle showed the presence of silver only at the particle surface before showing a pure copper inner core and thus this type of deposit is classified as bimetallic Cu/Ag. As mentioned previously, the exact depth of the silver surface is difficult to establish from FE-AES profiles as their sputtering rate is referenced to SiO_2. XPS

Table 2
Production and characterization of core-shell and bimetallic Cu/Ag particles by EDRR ($n = 20$), OCP value is an average of values after each cycle. All solutions contained 10 ppm Ag.

Deposition potential vs. Ag/AgCl (V)	Deposition time (ms)	Replacement time (s)	Stirring (rpm)	EDS, Cu:Ag (wt%-ratio)	XPS, Cu:Ag (wt%-ratio)	Deposit size (nm)	Average OCP vs. Ag/AgCl (mV)
−0.1	500	2	–	121	Pure Cu	539 ± 106	67 ± 1
−0.1	500	50	–	6	Bimetallic Cu/Ag (0.2)	207 ± 88 nm	126 ± 73
−0.1	500	50	300	0.02	Pure Ag	330 ± 142	299 ± 1
−0.1	500	100	–	0.02	Pure Ag	270 ± 74	282 ± 9
−0.5	500	2	–	174	Pure Cu	817 ± 191	58 ± 1
−0.5	500	50	–	33	Pure Ag	837 ± 323	67 ± 1
−0.5	500	300	–	9	Bimetallic Cu/Ag (0.5)	843 ± 313	73 ± 3
−0.5	50	2	–	164	Pure Cu	840 ± 227	65 ± 3
−0.5	50	50	–	34	Bimetallic Cu/Ag (1.2)	637 ± 144	69 ± 2
−0.5	50	150	–	0.01	Pure Ag	211 ± 62	212 ± 85

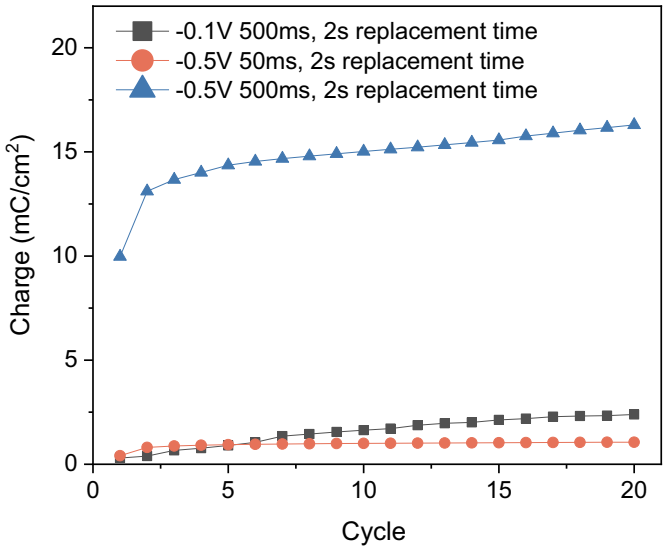

Fig. 8. Evolution of deposition charge during EDRR processes in copper process solution with [Ag] = 10 ppm.

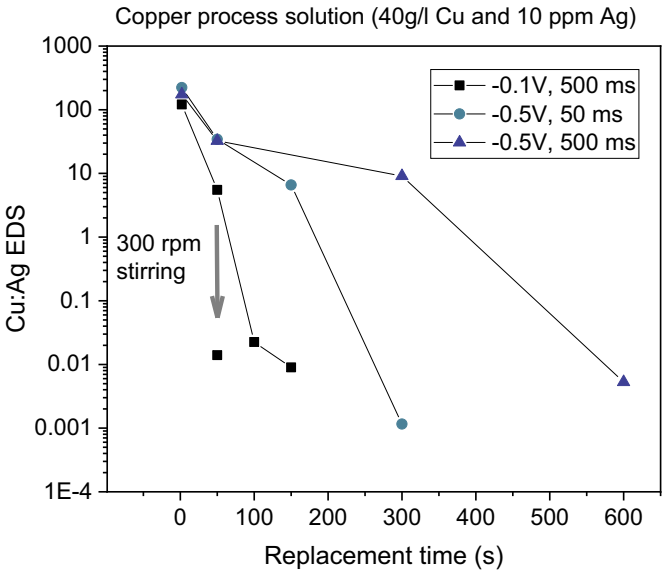

Fig. 9. Cu:Ag wt%-ratios of deposits from copper process solution with [Ag] = 10 ppm by EDRR (n = 20) under different deposition parameters.

analysis of large areas of the same sample showed a similar result with both Ag and Cu being present at the sample surface. Importantly, no oxygen could be detected at the outer silver containing surface or in the inner copper core.

The compiled results of EDRR from the copper process solution with 1 ppm Ag are reported in the supplementary information (Fig. S3 and Table S1). The results from those experiments followed the same general trends observed for the 10 ppm Ag solution: silver content and OCP values increased with higher replacement times. After redox replacement, the obtained pure silver particles were slightly smaller or the same size (ca. 110 nm) as from the solution with 10 ppm Ag. This result shows that the EDRR method with the investigated parameters is applicable for the creation of a CNT film surface functionalized with pure Ag particles and Cu/Ag deposits from solutions where the concentration of copper (40 g/L) is up to 40,000 times higher than the amount of silver (1 ppm).

3.4. Open-circuit potential transients during EDRR

Pure copper and silver have different electrode potentials as shown in Eq. (3) and therefore the differences in the CNT film surface composition during and after redox replacement can be observed from the open circuit potential (OCP) transients recorded directly following the copper deposition pulse, shown in Fig. 11. This reasoning is also supported by the experimental data shown in Tables 1 and 2, where the silver loading from EDS analysis increases with the OCP values and replacement time. The slope of the OCP transient at a given moment during redox replacement reflects the kinetics of the replacement reaction. For the purposes of analyzing the OCP transients the actual potentials of pure silver and pure copper deposits can be seen from Tables 1 and 2, respectively. The potential of pure copper deposits on the CNT film is calculated as the average of Table 2 values at 2 s replacement time at OCP = 63 mV vs. Ag/AgCl. The potential of pure silver deposits on the CNT film is calculated as the average of Table 1 values (from the values of highly pure Ag particles formed by EDRR) at OCP = 290 mV vs. Ag/AgCl. The dashed lines in Fig. 11 represent these potentials of pure copper and silver particles and are used to classify the evolution of the OCP transients in different stages, depending on the chemical composition of the deposits on the surface of the CNT film. In Stage I, right after the electrodeposition pulse, the deposits are pure copper (Cu/Ag wt%- ratio of > 121 from Table 2). In Stage II, redox replacement takes place at the surfaces of copper particles and thus the OCP value rises with time while reflecting the mixed potential between copper and silver. In Stage III the particles have been transformed into highly pure silver with very small concentration of Cu remaining (ca. 0.1–1% by EDS, depending on the employed deposition parameters and replacement time). OCP transients for samples with a deposition pulse of −0.1 V vs. Ag/AgCl for 500 ms and replacement times of 50 s and 150 s for 20 cycles are shown in Fig. 11. For the sake of clarity, only the first, fifth and last OCP transient during EDRR are shown.

The obtained OCP transients in Fig. 11 can be explained as following: When the replacement time is set to 150 s without stirring or 50 s with stirring, the redox replacement process fully proceeds into Stage III during all cycles and the surface of the CNT film consists of highly pure Ag deposits after each cycle. In other words, enough Ag has been transferred from the solution to the particle surfaces in order for all of the deposited Cu to be replaced by Ag. In the beginning of the redox replacement reaction, the whole copper particle surface is available and thus the kinetics of the replacement reaction are fast [32]. This is reflected by the steep rise in potential after ca. 20 s in Stage II as silver covers more and more of the copper deposit surfaces. The potential then begins to stabilize at higher replacement times near Stage III as the silver deposits reach a high degree of purity. The general shapes of the OCP transients are similar to those typically seen in SLRR processes, where individual monolayers of atoms are being replaced [14–18,20].

The results for the sample with 50 s replacement time and no stirring are markedly different. For this sample the final recorded OCP values during all cycles are within Stage II, corresponding with a mixed surface potential of copper and silver. From the previously shown XPS results (Table 2) and FE-AES depth profiles (Fig. 10) of the sample it is known that these deposits are both bimetallic and core-shell structured. Analysis of the OCP data shows that during the first 6 cycles the transients exhibit similar behavior as the sample with 150 s replacement time, with a steep rise in potential after an induction period of ca. 20 s. However, the potential never reaches values in Stage III and all the formed deposits contain both silver and copper. After the first 6 cycles the OCP transients are still within Stage II, but show a smaller rise in potential with time, i.e. the speed at which redox replacement is taking place slows down. This decrease could be due to diffusion limitations during the short replacement time due to small concentration of noble Ag, similar to results with the SLRR method [15]. Thus, with a replacement time of 150 s the silver ions have enough time to diffuse to

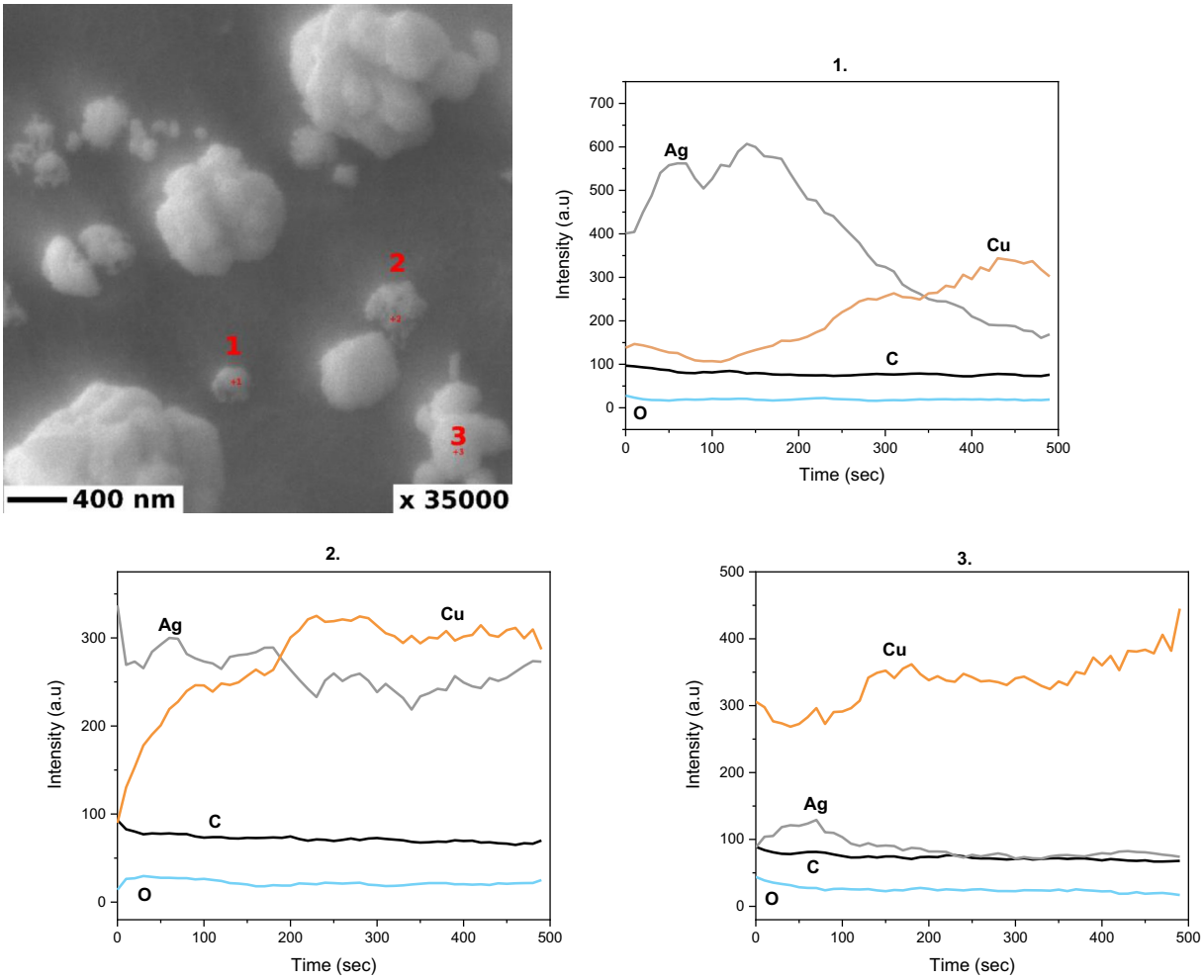

Fig. 10. Field emission Auger electron spectroscopy depth profiles of bimetallic particles from copper process solution with [Ag] = 10 ppm with parameters of −0.1 V vs. Ag/AgCl for 500 ms and replacement time of 50 s (n = 20).

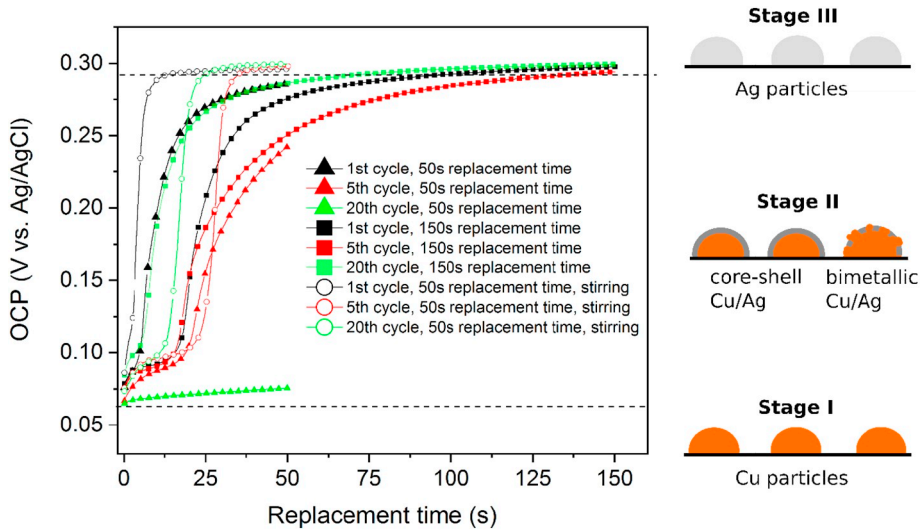

Fig. 11. Open circuit potential transients during EDRR in copper process solution with [Ag] = 10 ppm with deposition pulse of −0.1 V vs. Ag/AgCl for 500 ms during 1st, 5th and 20th cycles for samples with replacement time of 50 s and 150 s.

the CNT film surface during all cycles. Conversely, with a replacement time of 50 s the vicinity of the electrode surface is depleted of silver ions during the first 6 cycles. Thus, after this point the diffusion of silver ions to the CNT film surface becomes the rate-limiting step in the redox replacement reaction between copper and silver.

The results suggest that the progress of the EDRR process could also be observed by the open circuit potential, which indicates the in-situ deposit composition on the CNT film during EDRR. For a further study

of EDRR in the Cu−Ag system the experiments could be controlled by potential limits instead of replacement time during the redox replacement step.

4. Conclusions

The electrodeposition-redox replacement method was investigated to control the deposition of pure silver and bimetallic copper/silver particles onto a carbon nanotube film. The utilized solutions simulated industrial copper electrolysis solutions with 1–10 ppm Ag, 40 g/L of Cu and 120 g/L sulphuric acid. With this method, first an electrodeposition pulse was applied to produce highly pure copper particles. The cell was then set to open circuit potential conditions and redox replacement took place between the solid copper particles and silver ions in the solution. Three different deposition conditions of −0.1 V for 500 ms, −0.5 V for 50 ms and −0.5 V for 500 ms vs. Ag/AgCl were used and the redox replacement times at open circuit potential were varied between 2 and 600 s. With 20 cycles of deposition and redox replacement, the carbon nanotube film surface could be tailored with a variety of Cu/Ag deposit compositions, or pure silver particles.

The composition of the particles could be controlled from pure copper to copper core-silver shell to pure silver particles by controlling the redox replacement time. Moreover, the progression of the replacement was also observed from the open circuit potential transient during the experiment. When applying stirring the EDRR process was considerably faster with the deposits showing a higher degree of agglomeration. Silver particles with up to 99.9% purity and ca. 100 nm diameter could be formed with deposition conditions of −0.5 V vs. Ag/AgCl for 50 ms and 300 s of replacement time. The EDRR method for recovery of pure silver particles from the copper process solution with 10 ppm Ag was shown to be > 7 times more efficient than by traditional cementation in the same solution.

Various types of bimetallic copper-silver particles could be produced with the method as well. For example, copper core-silver shell nanoparticles ca. 250 nm in diameter with a copper to silver ratio of 6 could be deposited with the conditions of −0.1 V for 500 ms with 50 s replacement time. With a higher applied charge of −0.5 V for 500 ms and 50 s replacement time, the core-shell particles were ca. 840 nm in diameter with a copper to silver ratio of 33. In summary, this paper shows the versatile nature of the electrodeposition-redox replacement method to control the composition of bimetallic Cu/Ag and pure Ag particles. The method could be applied to energy efficiently recover homogeneously distributed high purity silver deposits or to create a surface of desired Cu/Ag composition directly on the employed carbon nanotube film from solutions containing industrially relevant concentration ranges (dilute Ag concentration and high Cu concentration).

Acknowledgements

This work has been financed by the Finnish Academy NoWaste project (grant number 297962). RawMatTERS Finland Infrastructure (RAMI) supported by Academy of Finland is greatly acknowledged. Marc Raes is acknowledged for FE-SEM imaging and EDS analysis. Priya Laha is acknowledged for the FE-AES analysis. M.L acknowledges the Association of Finnish Steel and Metal producers METSEK project. D.J. thanks National Science Center, Poland (under the Polonez program, grant agreement UMO-2015/19/P/ST5/03799) and the European Union's Horizon 2020 research and innovation programme (Marie Sklodowska-Curie grant agreement 665778). D.J. would also like to acknowledge the Ministry for Science and Higher Education for the scholarship for outstanding young scientists (0388/E-367/STYP/12/2017). S.P. acknowledges financial support by Research Foundation Flanders (FWO) under project number SB-19-151.

Appendix A. Supplementary data

Supplementary data to this article can be found online at https://doi.org/10.1016/j.surfcoat.2019.05.085.

References

[1] W.G. Davenport, M.J. King, M.E. Schlesinger, A.K. Biswas, Extractive Metallurgy of Copper, Elsevier, 2002.
[2] G. Sulka, M. Jaskuła, Effect of sulphuric acid and copper sulphate concentrations on the morphology of silver deposit in the cementation process, Electrochim. Acta 51 (2006) 6111–6119.
[3] G. Sulka, M. Jaskuła, Study of the mechanism of silver ions cementation onto copper from acidic sulphate solutions and the morphology of the silver deposit, Hydrometallurgy 72 (2004) 93–110.
[4] O. Keleş, An optimization study on the cementation of silver with copper in nitrate solutions by Taguchi design, Hydrometallurgy 95 (2009) 333–336.
[5] S. Ju, Y. Zhang, Y. Zhang, P. Xue, Y. Wang, Clean hydrometallurgical route to recover zinc, silver, lead, copper, cadmium and iron from hazardous jarosite residues produced during zinc hydrometallurgy, J. Hazard. Mater. 192 (2011) 554–558.
[6] J.P. Chen, L.L. Lim, Key factors in chemical reduction by hydrazine for recovery of precious metals, Chemosphere 49 (2002) 363–370.
[7] I. Rivera, A. Roca, M. Cruells, F. Patiño, E. Salinas, Study of silver precipitation in thiosulfate solutions using sodium dithionite. Application to an industrial effluent, Hydrometallurgy 89 (2007) 89–98.
[8] J. Hanzlík, J. Jehlička, O. Šebek, Z. Weishauptová, V. Machovič, Multi-component adsorption of Ag(I), Cd(II) and Cu(II) by natural carbonaceous materials, Water Res. 38 (2004) 2178–2184.
[9] N. Othman, H. Mat, M. Goto, Separation of silver from photographic wastes by emulsion liquid membrane system, J. Membr. Sci. 282 (2006) 171–177.
[10] M. Chatelut, E. Gobert, O. Vittori, Silver electrowinning from photographic fixing solutions using zirconium cathode, Hydrometallurgy 54 (2000) 79–90.
[11] V. Reyes-Cruz, C. Ponce-de-León, I. González, M.T. Oropeza, Electrochemical deposition of silver and gold from cyanide leaching solutions, Hydrometallurgy 65 (2002) 187–203.
[12] J.P. Chen, L. Lim, Recovery of precious metals by an electrochemical deposition method, Chemosphere 60 (2005) 1384–1392.
[13] F. Fu, Q. Wang, Removal of heavy metal ions from wastewaters: a review, J. Environ. Manag. 92 (2011) 407–418.
[14] C. Thambidurai, Y. Kim, J.L. Stickney, Electrodeposition of Ru by atomic layer deposition (ALD), Electrochim. Acta 53 (2008) 6157–6164.
[15] C. Thambidurai, D.K. Gebregziabiher, X. Liang, Q. Zhang, V. Ivanova, P. Haumesser, J.L. Stickney, E-ALD of Cu nanofilms on Ru/Ta wafers using surface limited redox replacement, J. Electrochem. Soc. 157 (2010) D466–D471.
[16] N. Dimitrov, Recent advances in the growth of metals, alloys, and multilayers by surface limited redox replacement (SLRR) based approaches, Electrochim. Acta 209 (2016) 599–622.
[17] N. Jayaraju, D. Vairavapandian, Y.G. Kim, D. Banga, J.L. Stickney, Electrochemical atomic layer deposition (E-ALD) of Pt nanofilms using SLRR cycles, J. Electrochem. Soc. 159 (2012) D616–D622.
[18] N. Jayaraju, D. Banga, C. Thambidurai, X. Liang, Y.G. Kim, J.L. Stickney, PtRu nanofilm formation by electrochemical atomic layer deposition (E-ALD), Langmuir 30 (2014) 3254–3263.
[19] C. Mitchell, M. Fayette, N. Dimitrov, Homo-and hetero-epitaxial deposition of Au by surface limited redox replacement of Pb underpotentially deposited layer in one-cell configuration, Electrochim. Acta 85 (2012) 450–458.
[20] M. Fayette, Y. Liu, D. Bertrand, J. Nutariya, N. Vasiljevic, N. Dimitrov, From Au to Pt via surface limited redox replacement of Pb UPD in one-cell configuration, Langmuir 27 (2011) 5650–5658.
[21] K. Yliniemi, N.T. Nguyen, S. Mohajernia, N. Liu, B.P. Wilson, P. Schmuki, M. Lundström, A direct synthesis of platinum/nickel co-catalysts on titanium dioxide nanotube surface from hydrometallurgical-type process streams, J. Clean. Prod. 201 (2018) 39–48.
[22] I. Korolev, P. Altınkaya, P. Halli, P. Hannula, K. Yliniemi, M. Lundström, Electrochemical recovery of minor concentrations of gold from cyanide-free cupric chloride leaching solutions, J. Clean. Prod.
[23] K. Yliniemi, P. Halli, I. Korolev, Z. Wang, P. Hannula, M. Lundström, Effect of Impurities in Precious Metal Recovery by Electrodeposition-Redox Replacement Method from Industrial Side-Streams and Process Streams, 85(4) (2018), pp. 59–67.
[24] H.T. Hai, J.G. Ahn, D.J. Kim, J.R. Lee, H.S. Chung, C.O. Kim, Developing process for coating copper particles with silver by electroless plating method, Surf. Coat. Technol. 201 (2006) 3788–3792.
[25] I. Kim, K. Woo, Z. Zhong, E. Lee, D. Kang, S. Jeong, Y.-M. Choi, Y. Jang, S. Kwon, J. Moon, Selective light-induced patterning of carbon nanotube/silver nanoparticle composite to produce extremely flexible conductive electrodes, ACS Appl. Mater. Interfaces 9 (2017) 6163–6170.
[26] N.R. Kim, K. Shin, I. Jung, M. Shim, H.M. Lee, Ag–Cu bimetallic nanoparticles with enhanced resistance to oxidation: a combined experimental and theoretical study, J. Phys. Chem. C 118 (2014) 26324–26331.
[27] Y. Peng, C. Yang, K. Chen, S.R. Popuri, C. Lee, B. Tang, Study on synthesis of ultrafine Cu–Ag core–shell powders with high electrical conductivity, Appl. Surf. Sci. 263 (2012) 38–44.
[28] J. Zhao, D. Zhang, X. Song, Simple and eco-friendly preparation of silver films coated on copper surface by replacement reaction, Appl. Surf. Sci. 258 (2012)

7430–7434.
[29] Y. Jin, F. Chen, Facile preparation of Ag-Cu bifunctional electrocatalysts for zinc-air batteries, Electrochim. Acta 158 (2015) 437–445.
[30] Y. Jin, F. Chen, Y. Lei, X. Wu, A silver-copper alloy as an oxygen reduction electrocatalyst for an advanced zinc-air battery, ChemCatChem 7 (2015) 2377–2383.
[31] K. Shin, D.H. Kim, H.M. Lee, Catalytic characteristics of AgCu bimetallic nanoparticles in the oxygen reduction reaction, ChemSusChem 6 (2013) 1044–1049.
[32] C. Durante, V. Perazzolo, L. Perini, M. Favaro, G. Granozzi, A. Gennaro, Electrochemical activation of carbon–halogen bonds: electrocatalysis at silver/copper nanoparticles, Appl. Catal. B Environ. 158 (2014) 286–295.
[33] G. Yang, G. Gao, C. Wang, C. Xu, H. Li, Controllable deposition of Ag nanoparticles on carbon nanotubes as a catalyst for hydrazine oxidation, Carbon 46 (2008) 747–752.
[34] W. Yuan, G. Jiang, J. Che, X. Qi, R. Xu, M.W. Chang, Y. Chen, S.Y. Lim, J. Dai, M.B. Chan-Park, Deposition of silver nanoparticles on multiwalled carbon nanotubes grafted with hyperbranched poly (amidoamine) and their antimicrobial effects, J. Phys. Chem. C 112 (2008) 18754–18759.
[35] M. Valodkar, S. Modi, A. Pal, S. Thakore, Synthesis and anti-bacterial activity of Cu, Ag and Cu–Ag alloy nanoparticles: a green approach, Mater. Res. Bull. 46 (2011) 384–389.
[36] Z. Li, L. Fan, T. Zhang, K. Li, Facile synthesis of Ag nanoparticles supported on MWCNTs with favorable stability and their bactericidal properties, J. Hazard. Mater. 187 (2011) 466–472.
[37] C. Rousse, J. Josse, V. Mancier, S. Levi, S.C. Gangloff, P. Fricoteaux, Synthesis of copper–silver bimetallic nanopowders for a biomedical approach; study of their antibacterial properties, RSC Adv. 6 (2016) 50933–50940.
[38] A. Yu, Q. Wang, J. Yong, P.J. Mahon, F. Malherbe, F. Wang, H. Zhang, J. Wang, Silver nanoparticle–carbon nanotube hybrid films: preparation and electrochemical sensing, Electrochim. Acta 74 (2012) 111–116.
[39] H. Bagheri, A. Hajian, M. Rezaei, A. Shirzadmehr, Composite of Cu metal nanoparticles-multiwall carbon nanotubes-reduced graphene oxide as a novel and high performance platform of the electrochemical sensor for simultaneous determination of nitrite and nitrate, J. Hazard. Mater. 324 (2017) 762–772.
[40] P. Ai, M. Tan, Y. Ishikuro, Y. Hosoi, G. Yang, Y. Yoneyama, N. Tsubaki, Design of an autoreduced copper in carbon nanotube catalyst to realize the precisely selective hydrogenation of dimethyl oxalate, ChemCatChem 9 (2017) 1067–1075.
[41] P. Hannula, A. Peltonen, J. Aromaa, D. Janas, M. Lundström, B.P. Wilson, K. Koziol, O. Forsén, Carbon nanotube-copper composites by electrodeposition on carbon nanotube fibers, Carbon 107 (2016) 281–287.
[42] S.M. Uddin, T. Mahmud, C. Wolf, C. Glanz, I. Kolaric, C. Volkmer, H. Höller, U. Wienecke, S. Roth, H.-J. Fecht, Effect of size and shape of metal particles to improve hardness and electrical properties of carbon nanotube reinforced copper and copper alloy composites, Compos. Sci. Technol. 70 (2010) 2253–2257.
[43] R. Sundaram, T. Yamada, K. Hata, A. Sekiguchi, Electrical performance of lightweight CNT-cu composite wires impacted by surface and internal Cu spatial distribution, Sci. Rep. 7 (2017) 9267.
[44] C.K. Kim, G. Lee, M.K. Lee, C.K. Rhee, A novel method to prepare Cu@Ag core–shell nanoparticles for printed flexible electronics, Powder Technol. 263 (2014) 1–6.
[45] A. Lekawa-Raus, P. Haladyj, K. Koziol, Carbon nanotube fiber–silver hybrid electrical conductors, Mater. Lett. 133 (2014) 186–189.
[46] S. Seisko, J. Aromaa, P. Latostenmaa, O. Forsen, B. Wilson, M. Lundstrom, Pressure leaching of decopperized copper electrorefining anode slimes in strong acid solution, Physicochem. Problems Min. Proc. 53 (2017).
[47] D. Janas, M. Rdest, K.K.K. Koziol, Free-standing films from chirality-controlled carbon nanotubes, Mater. Des. 121 (2017) 119–125.
[48] G. Stando, D. Łukawski, F. Lisiecki, D. Janas, Intrinsic hydrophilic character of carbon nanotube networks, Appl. Surf. Sci. 463 (2019) 227–233.
[49] D. Janas, G. Stando, Unexpectedly strong hydrophilic character of free-standing thin films from carbon nanotubes, Sci. Rep. 7 (2017) 12274.
[50] P. Hannula, J. Aromaa, B.P. Wilson, D. Janas, K. Koziol, O. Forsén, M. Lundström, Observations of copper deposition on functionalized carbon nanotube films, Electrochim. Acta 232 (2017) 495–504.
[51] X. Wang, P. Huang, L. Feng, M. He, S. Guo, G. Shen, D. Cui, Green controllable synthesis of silver nanomaterials on graphene oxide sheets via spontaneous reduction, RSC Adv. 2 (2012) 3816–3822.
[52] V. Mancier, C. Rousse-Bertrand, J. Dille, J. Michel, P. Fricoteaux, Sono and electrochemical synthesis and characterization of copper core–silver shell nanoparticles, Ultrason. Sonochem. 17 (2010) 690–696.
[53] L. Huang, E. Lee, K. Kim, Electrodeposition of monodisperse copper nanoparticles on highly oriented pyrolytic graphite electrode with modulation potential method, Colloids Surf. A Physicochem. Eng. Asp. 262 (2005) 125–131.
[54] X. Zhao, A. Harmer, N. Heinig, K. Leung, Parametric study on electrochemical deposition of copper nanoparticles on an ultrathin polypyrrole film deposited on a gold film electrode, Langmuir 20 (2004) 5109–5113.
[55] G.W. Tindall, S. Bruckenstein, The simultaneous determination by stripping analysis of copper and silver in sulfuric acid supporting electrolyte using the platinum ring-disk electrode, J. Electroanal. Chem. Interfacial Electrochem. 22 (1969) 367–373.
[56] K. Yliniemi, D. Wragg, B.P. Wilson, H.N. McMurray, D.A. Worsley, P. Schmuki, K. Kontturi, Formation of Pt/Pb nanoparticles by electrodeposition and redox replacement cycles on fluorine doped tin oxide glass, Electrochim. Acta 88 (2013) 278–286.